

**Response to**

**Request for Additional Information No. 167, Supplement 1**

**1/23/2009**

**U. S. EPR Standard Design Certification**

**AREVA NP Inc.**

**Docket No. 52-020**

**SRP Section: 15.03.01-15.03.02 - Loss of Forced Reactor Coolant Flow Including  
Trip of Pump Motor and Flow Controller Malfunctions**

**SRP Section: 15.03.03-15.03.04 - Reactor Coolant Pump Rotor Seizure and  
Reactor Coolant Pump Shaft Break**

**SRP Section: 15.06.05 - Loss of Coolant Accidents Resulting From Spectrum of  
Postulated Piping Breaks Within the Reactor Coolant Pressure Boundary**

**Application Section: FSAR Ch 15**

**QUESTIONS for Reactor System, Nuclear Performance and Code Review (SRSB)**

**Question 15.06.05-28:**

Explain the reactor coolant pump (RCP) trip logic and required operator actions should a small break loss of coolant accident occur. Show that the RCP trip will occur in a timely manner such that heat transfer is maximized while coolant mass loss is minimized. Explain how RCP seals are protected. Show that the RCPs will not be inadvertently tripped during a steam generator tube rupture event. Provide emergency procedure guidelines, intended criteria and proposed ITAAC related to operator actions for RCP trip. This question is asked to satisfy requirement of GDC 35, "Emergency Core Cooling."

**Response to Question 15.06.05-28:**

The RCP trip is an automatic trip and does not require operator action. The trip utilizes the differential pressure ( $\Delta P$ ) across the RCPs to indicate the presence of two-phase flow. When one of two  $\Delta P$  measurements from two of the four RCPs is below the setpoint, and a safety injection (SI) signal is present, the RCPs will trip. The trip setpoint is 80 percent of the initial  $\Delta P$  across the pump. The requirement for the presence of an SI signal reduces the possibility of a spurious RCP trip. The functional logic for automatic actuation of RCP trip is shown in U.S. EPR FSAR Tier 2, Figure 7.3-27.

The purpose of the RCP trip is to prevent the forced convection of two-phase flow. This would result in more mass lost out the break, and if the RCPs are subsequently stopped, the two phases would separate and, due to insufficient liquid inventory, inadequate core cooling (ICC) could occur. The trip is designed to stop the RCPs early when the void fraction is still relatively low. The setpoints for the trip have been evaluated to verify that they trip the RCPs soon enough to provide adequate protection, but not in undesired situations.

The analysis results for a non-loss of offsite power (LOOP),  $\Delta P$  trip, small break loss of coolant accident (SBLOCA) break spectrum are presented in U.S. EPR FSAR Tier 2, Section 15.6.5.2.3. The results show that the trip occurs before reaching the minimum RCS inventory and is adequate to satisfy 10 CFR 50.46 criteria. For these non-LOOP,  $\Delta P$  trip, SBLOCA cases, the setpoint is conservatively biased low to allow for longer operation of the RCPs. With the smaller breaks, the pumps run slightly longer than if the pumps are lost at LOOP concurrent with reactor trip (RT). This, in combination with lack of emergency feedwater (EFW) (which is not signaled because LOOP has not occurred and the steam generator (SG) level remains above the setpoint), increases the peak cladding temperature (PCT) relative to the LOOP cases for the smallest small breaks.

However, as break size increases, the void fraction decreases faster, the  $\Delta P$  across the pump increases faster, and the time between RT and RCP trip decreases. Additionally, Table 15.06.05-28-1 shows system conditions at the time of and shortly after the time of the RCP  $\Delta P$  trip for both the smallest break size and the limiting PCT break size of the non-LOOP break spectrum. This information is representative of the conditions at the time of RCP trip across the break spectrum: low power, a slightly decreased primary temperature, and a decreased primary pressure. Prior to RCP trip, the void fraction in the pump is increasing. At the time of the RCP  $\Delta P$  trip, the void fraction is 0.17. After the time of RCP trip, the flow through the pump returns to a single-phase liquid. At the time of the RCP trip, the inventory in the core is above 90 percent of the initial inventory, which allows for adequate heat transfer from the rods to the coolant.

Figure 15.06.05-28-1 shows that the RCPs do not inadvertently trip during a SG tube rupture (SGTR) event without LOOP. Throughout the transient, the RCP  $\Delta P$ s are above the maximized setpoint (80 percent + uncertainty = 83 percent). Additionally, the RCP trip requires the presence of the SI signal. At the beginning of the transient the RCP  $\Delta P$  is decreasing; however, even if the setpoint is reached, the RCP trip would not occur because no SI signal is present. The actuation of SI on low pressurizer pressure also automatically initiates a partial cooldown of the RCS. The partial cooldown reduces the SG main steam relief train (MSRT) setpoints at a constant rate. With the reduction of SG pressure, the cold leg temperatures decrease and the densities increase. Because the RCP  $\Delta P$  is highly dependent on liquid density, following the SI signal, the RCP  $\Delta P$ s increase.

During normal operation, the RCP seals are provided with seal injection water from the chemical and volume control system (CVCS). The seal injection forces cool water down through the seals and into the RCS. During a SBLOCA without LOOP, the RCP trip results from the combination of the SI signal and the low  $\Delta P$  signal. The SI signal also causes stage one containment isolation, which isolates the CVCS letdown line but maintains the RCP seal injection and CVCS charging. For a larger break that results in a stage two containment isolation signal, the RCP seal injection and CVCS injection will be isolated (U.S. EPR FSAR Tier 2, Section 9.3.4.2.3.5). When seal injection is not available, the component cooling water system (CCWS) provides cooling to the thermal barrier of the RCP seals. Thermal barrier cooling does not automatically isolate due to an accident signal (U.S. EPR FSAR Tier 2, Section 9.2.2).

While the RCP  $\Delta P$  trip is fully automatic, the plant operator can manually trip individual RCPs. Furthermore, an additional automatic RCP trip signal is generated from the stage two containment isolation signal, discussed in U.S. EPR FSAR Tier 2, Section 7.3.1.2.9.

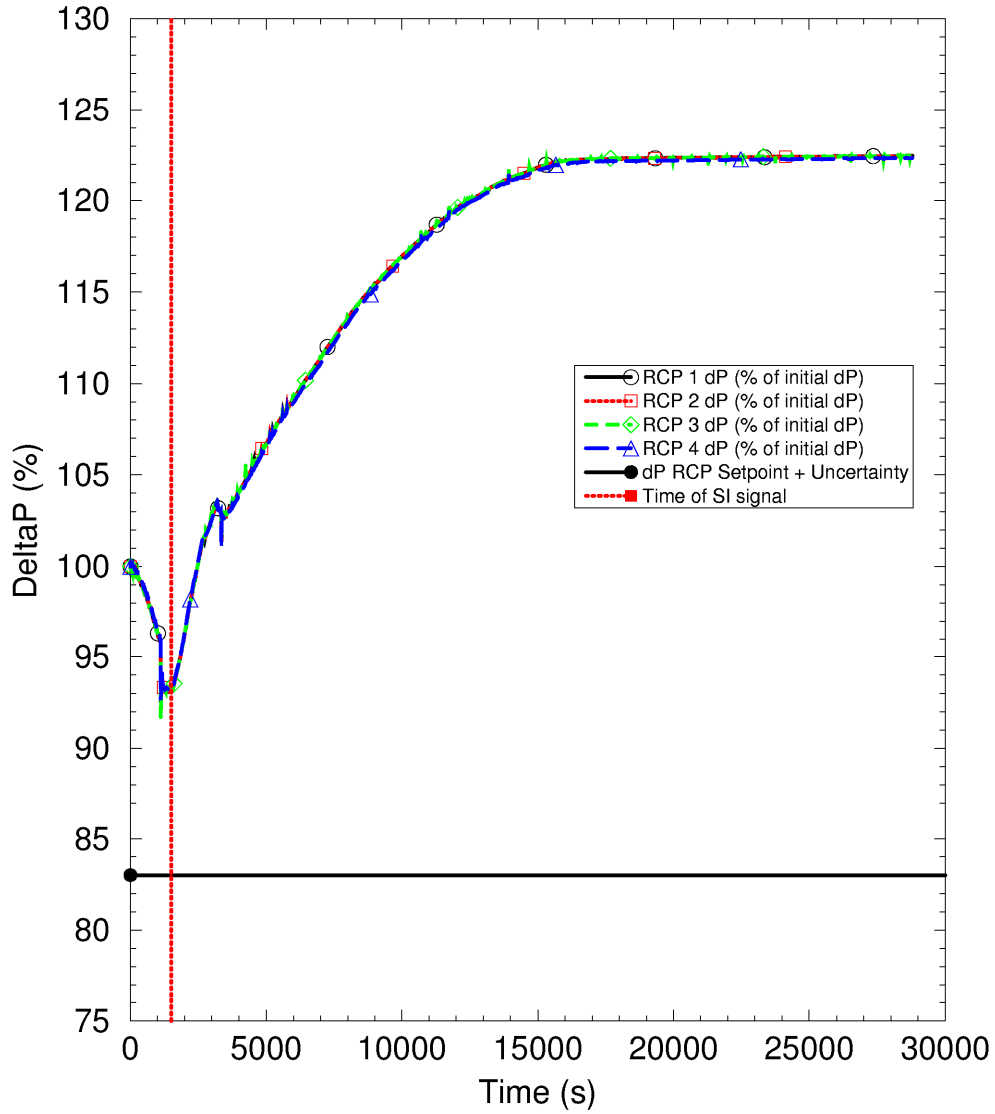
#### FSAR Impact:

The U.S. EPR FSAR will not be changed as a result of this question.

**Table 15.06.05-28-1—SBLOCA System Conditions at RCP  $\Delta P$  Trip**

Break Size	Time (sec)	Reactor Power (%)	Loop 4 RCP Velocity (rad/s)	Loop 4 Pump Void Fraction	RCS Tave (°F)	PZR Pressure (psia)	Vessel Inventory (% of Initial)
2.0 inch	686	2.84	122.1	0.17	567	1195	98.0
	790	2.73	0.00	0.00	563	1161	88.9
6.0 inch	64	5.21	122.1	0.17	579	1316	94.4
	174	3.88	0.00	0.00	581	1336	36.9

Figure 15.06.05-28-1—Non-LOOP SGTR RCP  $\Delta P$



**Question 15.06.05-38:**

Provide hot rod center line and volume average fuel temperature predictions as a function of burnup (both core average and hot rod burnup) for EPR fuel as predicted by RODEX3A/S-RELAP5 for RLBLOCA.

**Response to Question 15.06.05-38:**

The fuel rod temperatures were calculated at five times in the cycle for the limiting peak cladding temperature (PCT) case (i.e., Case 44) in the realistic large break loss of coolant accident (RLBLOCA) analysis of Topical Report ANP-10278P (Reference 1). The computational process is identical to the reference Case 44 computation except for the selected times in the cycle.

The RLBLOCA core modeling included in RODEX3A and S-RELAP5 for Case 44 consists of eight fuel rod types:

1. Hot UO<sub>2</sub> rod.
2. Hot assembly.
3. Hot ring (assemblies surrounding the hot assembly).
4. Average ring (core averaged fuel assembly).
5. Low-powered, outer ring (balance of core assemblies).
6. 2.0 percent Gadolinia (Gd) rod.
7. 4.0 percent Gd rod.
8. 8.0 percent Gd rod.

Rod types 1, 6, 7, and 8 are potential PCT rods (hot rods). The remaining rod types model the balance of the core and drive the thermal-hydraulic response of the system. The hot rods get their boundary conditions from the hot assembly.

Calculations of the fuel centerline (pellet inner radius) and volume average temperature are presented in the following tables and figures for the eight fuel rod types.

Table 15.06.05-38-1 presents the fuel rod average burnups for the eight fuel rod types at the five times in cycle. Table 15.06.05-38-1 is provided to explain the rod average burnups in the tabular data for maximum and volume average fuel (pellet) temperatures.

Table 15.06.05-38-2 and Table 15.06.05-38-3 present the maximum fuel centerline (inner radius) temperatures for the eight fuel rod types modeled in the RODEX3A/RELAP5 computations for Case 44. Figure 15.06.05-38-1 through Figure 15.06.05-38-8 show the axial distribution of fuel centerline (inner radius) temperatures. Table 15.06.05-38-4 and Table 15.06.05-38-5 present the volume average temperature for the eight fuel rod types modeled in the RODEX3A/RELAP5 computations for Case 44. Figure 15.06.05-38-9 through Figure 15.06.05-38-16 show the axial distribution of volume average fuel temperatures. These tables and figures show that the temperature variation is moderately affected by burnup and the trend is a decrease in temperatures with burnup.

Extending the steady state computation to the transient computation provides the PCT for each of the times in cycle. Table 15.06.05-38-6 shows the maximum cladding temperatures for the eight fuel rod types at the five times in cycle. The maximum cladding temperature of the eight fuel rod types for each burn up is shown in the bottom row. The largest difference of the maximum temperatures is approximately 81°F.

The PCT at the burnup of Case 44 (analysis of record) is 1425°F and the maximum cladding temperature rod for this case is the 4 percent Gd rod (see Table 15.06.05-38-6).

Figure 15.06.05-38-17 presents the data from Table 15.06.05-38-6 as a graph. The maximum cladding temperatures of the UO<sub>2</sub> fuel rods are moderately affected by the time in cycle and with a downward trend with increasing time in cycle. Gd bearing rods have lower initial stored energy at low burnup as compared to the UO<sub>2</sub> hot rod. As the Gd burns out, the maximum cladding behavior is similar to the hot UO<sub>2</sub> rod. The maximum cladding temperatures are moderately dependent on time in cycle (burnup) with a general downward trend, which is consistent with the initial steady state fuel rod temperatures.

In addition to the requested information, the RODEX3A/S-RELAP5 computations provide the steady state gap conductance and rod internal pressure for RLBLOCA Case 44 at five times in cycle and for the eight fuel rod types. Table 15.06.05-38-7 presents the rod internal pressure at five times in the cycle for the eight fuel rod types. The fuel rod gap conductance varies along the axial length. Table 15.06.05-38-8 and Table 15.06.05-38-9 show the axial maximum and axial average gap conductance at five times in the cycle. Figure 15.06.05-38-18 through Figure 15.06.05-38-25 present the axial distribution of gap conductance at five times in the cycle for the eight fuel rod types.

Figure 15.06.05-38-18, Figure 15.06.05-38-19, and Figure 15.06.05-38-20 show a progression of gap conductance for the hot rod, hot assembly, and surrounding assemblies as a function of burnup. With the exception of the highest burnup case, the gap conductance trend is the same for the hot rod, hot assembly, and surrounding assemblies. The hot assembly gap conductance behavior illustrated in the highest burnup case in Figure 15.06.05-38-19 is different from the surrounding assemblies and hot rod because the hot assembly is at an intermediate stage of burnup and gap closure. For this burnup, the hot rod has a closed gap over a significant part of its axial length; thus, it has a high gap conductance that is uniform over most of the axial length as shown in Figure 15.06.05-38-18. The closed gap of the hot rod is due to higher fast fluence and burnup than for the hot assembly rod. The rods of the surrounding assemblies have an open gap at the highest burnup and a lower gap conductance behavior that is uniform over its axial length as shown in Figure 15.06.05-38-20. The highest burnup hot assembly rod has a nonuniform gap conductance because it has a mix of closed, open, and partially closed gaps along its axial length as shown in Figure 15.06.05-38-19. The illustrated behavior is consistent with the modeling in RODEX3A, and the fuel rod data show the expected behavior for the various fuel types.

#### References for Question 15.06.05-38:

1. AREVA NP Topical Report ANP-10278P, Revision 0, "U.S. EPR Realistic Large Break Loss of Coolant Accident," AREVA NP Inc., March 2007.

**FSAR Impact:**

The U.S. EPR FSAR will not be changed as a result of this question.

**Table 15.06.05-38-1—Rod Average Burnups, Five Times in Cycle**

Time in Cycle (hours)	101	3039	6416	10131	13137
	Fuel Rod Average Burnups, GWd/MTU				
Hot UO2 Rod	0.22	6.71	14.25	22.50	28.90
Hot Assembly	0.20	6.00	12.86	20.49	26.56
Surrounding Assemblies	0.15	4.63	9.77	15.42	19.99
Core Average Assemblies	0.15	4.63	9.77	15.42	19.99
Outer Core Assemblies	0.15	4.63	9.77	15.42	19.99
2% Gd Rod	0.11	4.59	11.68	19.36	24.12
4% Gd Rod	0.10	3.81	10.17	17.85	23.93
8% Gd Rod	0.08	2.88	7.47	14.92	21.00

**Table 15.06.05-38-2—Maximum Fuel Rod Temperatures in Assemblies, Five Times in Cycle**

--	--	--

**Table 15.06.05-38-3—Maximum Hot Fuel Rod Temperatures, Five Times in Cycle**

--	--	--

**Table 15.06.05-38-4—Volume Average Fuel Rod Temperatures in Assemblies, Five Times in Cycle**

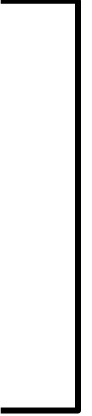


**Table 15.06.05-38-5—Volume Average Hot Fuel Rod Temperatures, Five Times in Cycle**

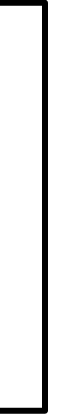


**Table 15.06.05-38-6—Maximum Cladding Temperatures, Five Times in Cycle**

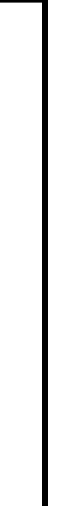




**Table 15.06.05-38-7—Fuel Rod Internal Gas Pressure, Five Times in Cycle**

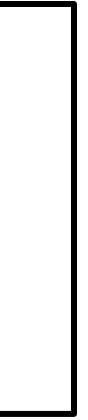


**Table 15.06.05-38-8—Fuel Rod Gap Conductance in Assemblies, Five Times in Cycle**

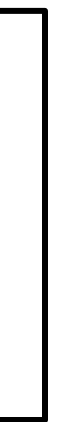


**Table 15.06.05-38-9—Hot Fuel Rod Gap Conductance, Five Times in Cycle**

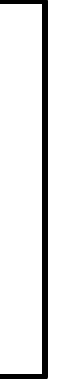


**Figure 15.06.05-38-1—Maximum Temperature, Hot UO<sub>2</sub> Rod, Five Burnups**



**Figure 15.06.05-38-2—Maximum Temperature, Hot Assembly UO<sub>2</sub> Rod, Five Burnups**



**Figure 15.06.05-38-3—Maximum Temperature, Surrounding Assemblies  
UO<sub>2</sub> Rod, Five Burnups**



**Figure 15.06.05-38-4—Maximum Temperature, Core Average Assemblies  
UO<sub>2</sub> Rod, Five Burnups**



**Figure 15.06.05-38-5—Maximum Temperature, Outer Core Assemblies UO<sub>2</sub>  
Rod, Five Burnups**



**Figure 15.06.05-38-6—Maximum Temperature, 2% Gd Rod, Five Burnups**



**Figure 15.06.05-38-7—Maximum Temperature, 4% Gd Rod, Five Burnups**





**Figure 15.06.05-38-8—Maximum Temperature, 8% Gd Rod, Five Burnups**



**Figure 15.06.05-38-9—Volume Average Temperature, Hot UO<sub>2</sub> Rod, Five Burnups**



**Figure 15.06.05-38-10—Volume Average Temperature, Hot Assembly UO<sub>2</sub>  
Rod, Five Burnups**



**Figure 15.06.05-38-11—Volume Average Temperature, Surrounding  
Assemblies UO<sub>2</sub> Rod, Five Burnups**



**Figure 15.06.05-38-12—Volume Average Temperature, Core Average  
Assemblies UO<sub>2</sub> Rod, Five Burnups**

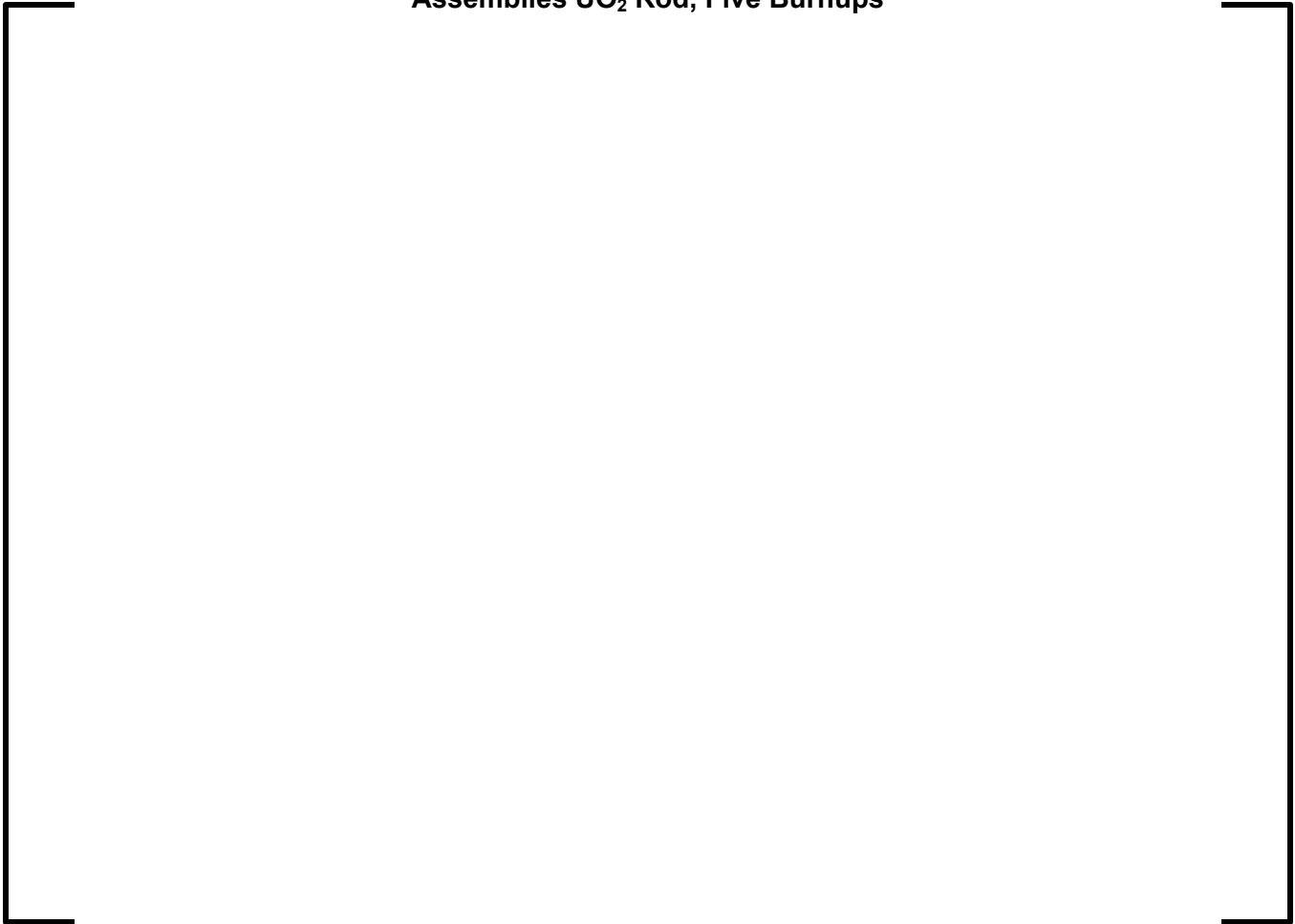


**Figure 15.06.05-38-13—Volume Average Temperature, Outer Core  
Assemblies UO<sub>2</sub> Rod, Five Burnups**

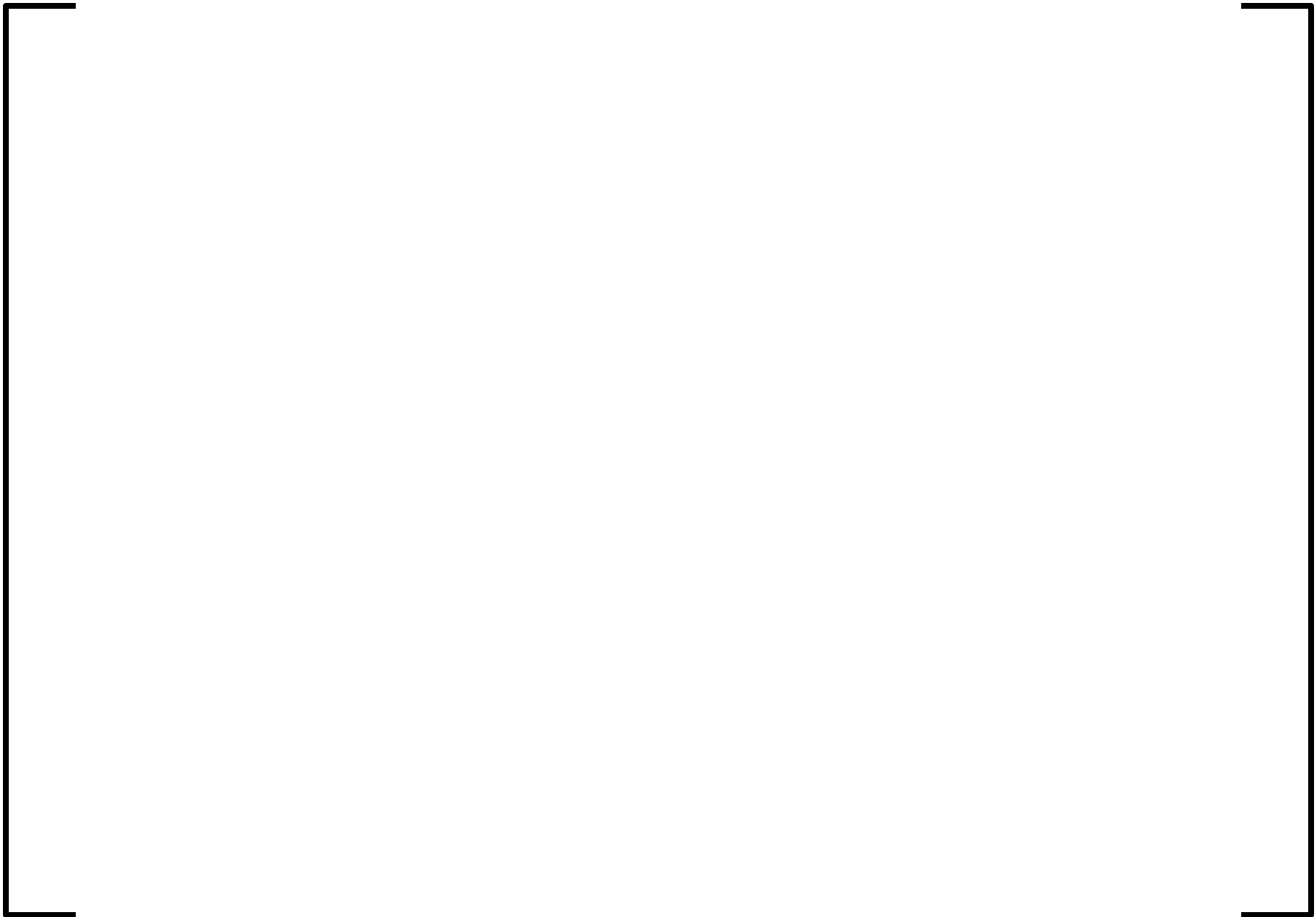


**Figure 15.06.05-38-14—Volume Average Temperature, 2% Gd Rod, Five Burnups**



**Figure 15.06.05-38-15—Volume Average Temperature, 4% Gd Rod, Five Burnups**





**Figure 15.06.05-38-16—Volume Average Temperature, 8% Gd Rod, Five Burnups**

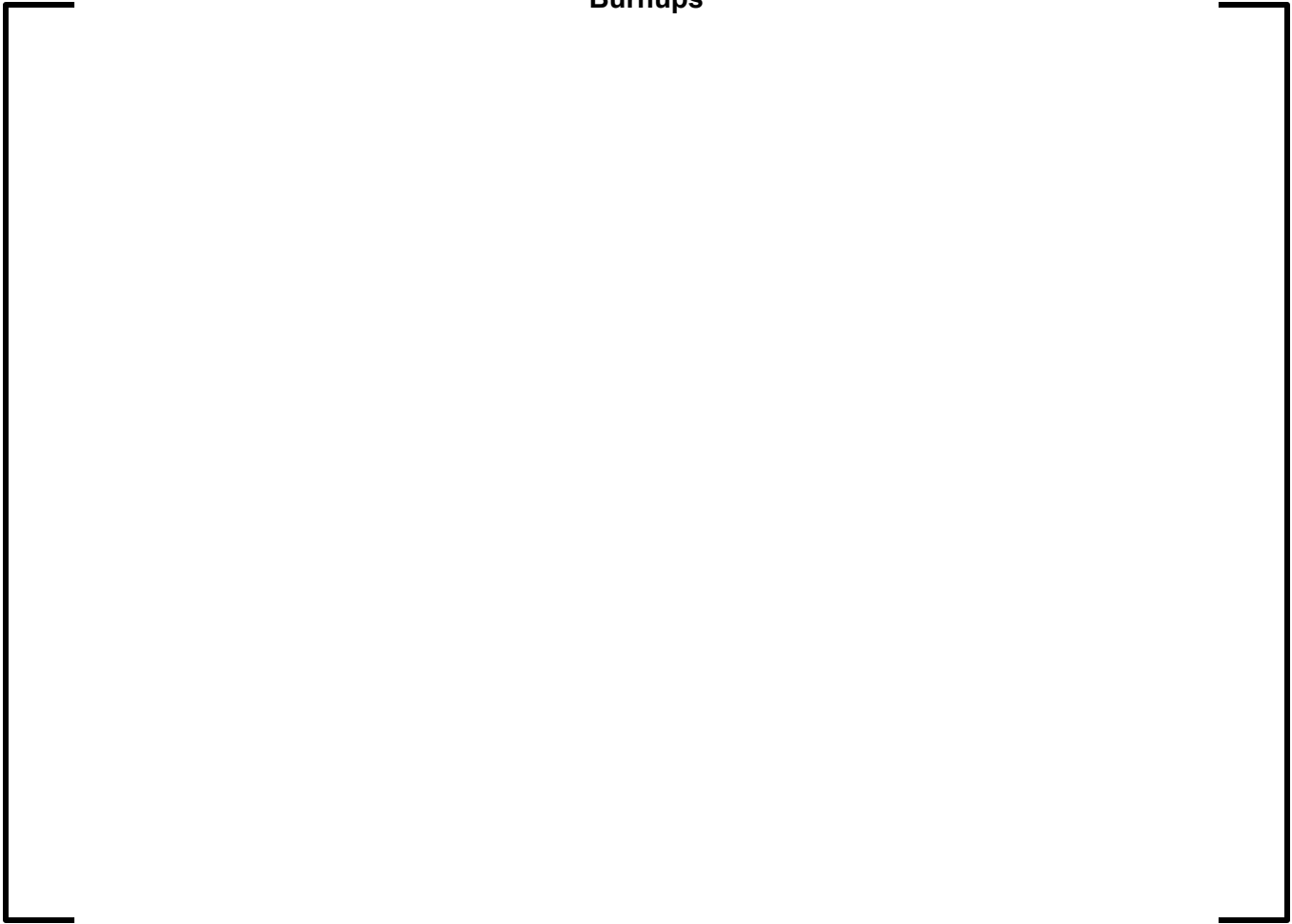


**Figure 15.06.05-38-17—Maximum Cladding Temperatures,  
Five Times in Cycle**



**Figure 15.06.05-38-18—Gap Conductance, Hot UO<sub>2</sub> Rod, Five Burnups**



**Figure 15.06.05-38-19—Gap Conductance, Hot Assembly UO<sub>2</sub> Rod, Five Burnups**



**Figure 15.06.05-38-20—Gap Conductance, Surrounding Assemblies UO<sub>2</sub>  
Rod, Five Burnups**

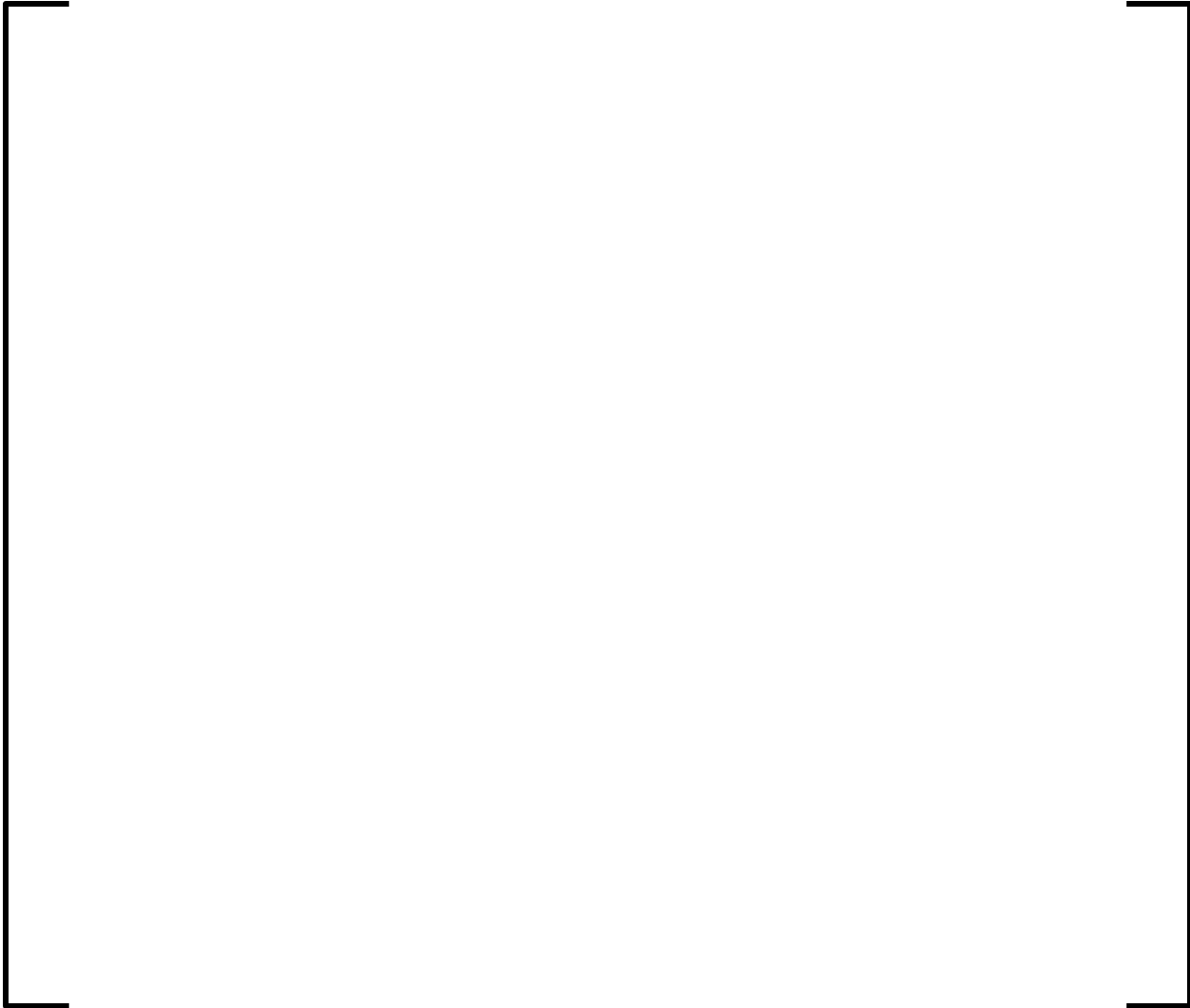


**Figure 15.06.05-38-21—Gap Conductance, Core Average Assemblies UO2  
Rod, Five Burnups**



**Figure 15.06.05-38-22—Gap Conductance, Outer Core Assemblies UO<sub>2</sub> Rod,  
Five Burnups**



**Figure 15.06.05-38-23—Gap Conductance, 2% Gd Rod, Five Burnups**

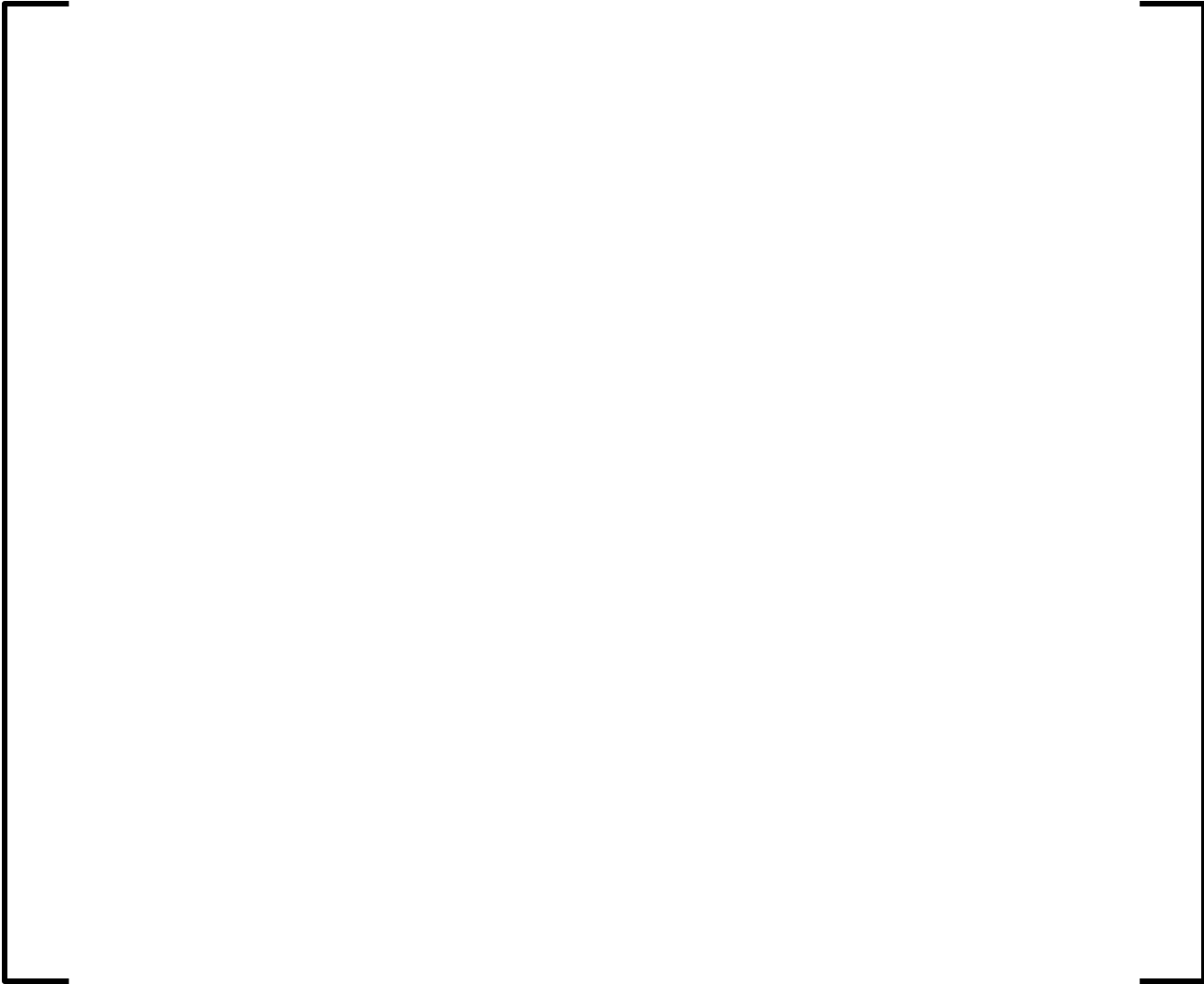




**Figure 15.06.05-38-24—Gap Conductance, 4% Gd Rod, Five Burnups**



**Figure 15.06.05-38-25—Gap Conductance, 8% Gd Rod, Five Burnups**



**Question 15.06.05-39:**

Explain the conservatism in accounting for burnup effects on fuel characteristics and initial stored energy and associated uncertainties in applying RODEX2/S-RELAP5 for SBLOCA analyses. Assess and demonstrate that the SBLOCA methodology accounts conservatively for the initial core stored energy particularly if the hot rod, hot assembly, inner and outer core initial fuel temperatures are under-predicted (see 15.06.05-42).

**Response to Question 15.06.05-39:**

The small break loss of coolant accident (SBLOCA) analyses presented in U.S. EPR FSAR Tier 2, Chapter 15 uses the NRC-approved computer code RODEX2-2A to calculate the fuel rod initial conditions, which are also used for the initialization of the S-RELAP5 calculations.

The fuel rod initial conditions are calculated at end-of-cycle (EOC) exposure. The EOC conditions are expected to result in the highest peak cladding temperature (PCT) for the SBLOCA events due to the top-skewed power profile, the higher fuel internal pressure, and the higher actinide decay heat characteristic of the EOC fuel exposure.

The S-RELAP5/RODEX2-2A method does not include a model to account for the burnup response of the fuel thermal-conductivity. Because the thermal-conductivity degrades with burnup, the code under-predicts the fuel initial stored energy at EOC conditions. However, the effect of the fuel stored energy on the SBLOCA results is negligible because most of the stored energy is dissipated before the PCT occurs for break sizes in the SBLOCA range. This is further discussed in the Response to Question 15.06.05-42.

**FSAR Impact:**

The U.S. EPR FSAR will not be changed as a result of this question.

**Question 15.06.05-41:**

Explain how the initial core stored energy is accounted for in performing transient analyses for the U.S. EPR. Is RODEX2 or RODEX3 used for other transient analyses other than for LOCA? If a separate code, such as COPERNIC, is used to determine the initial core fuel conditions, specify the parameters that are transferred to the system code used for transient analyses. In particular, explain how burnup effects on fuel characteristics and initial fuel-stored energy are taken into consideration. Discuss the fuel burnup related uncertainties applied to the transient analyses and the justification for these uncertainties in demonstrating the acceptability of the safety margins obtained.

**Response to Question 15.06.05-41:**

The initial fuel conditions used in performing transient analyses (other than loss of coolant accident) are based on the COPERNIC code output. The average rod fuel thermal conductivity, heat capacity, and gap coefficient (hgap) are parameters that are transferred to the system code (RELAP) used for transient analyses. RELAP models the average rod utilizing the parameters from COPERNIC to establish the initial fuel rod temperatures. This model is used during the transient to determine fuel temperature feedback and fuel rod surface heat flux. COPERNIC generates fuel rod characteristics as a function of fuel rod burn-up throughout the cycle. Parameters are selected to provide a conservative response depending on the transient. For example, during the transient, the reactivity contributions from moderator and fuel temperature changes are influenced by the fuel pellet-to-clad heat transfer coefficient (hgap). For fast transients, such as rod withdrawals from low power or subcritical conditions, where the fuel temperature feedback limits the peak power, a conservatively high hgap is assumed. For departure from nucleate boiling ratio (DNBR) related events, a high hgap is also conservative because it maximizes fuel rod surface heat flux. The exception is the loss of flow event. For the loss of flow event, sensitivity studies have shown that a low hgap results in a lower minimum DNBR (MDNBR) because the lower hgap keeps the heat flux higher later in the transient when the reactor coolant system (RCS) flow decreases. In the presence of a 0 pcm/°F moderator temperature coefficient for other heatup transients (e.g., turbine trip, loss of normal feedwater), a high hgap is conservative because it minimizes reactivity feedback from fuel temperature increase. The non-LOCA transient analysis uses a high hgap in all cases except loss of flow events where sensitivity analysis demonstrates that a low hgap is more conservative.

Portions of the response were added to U.S. EPR FSAR Tier 2, Section 15.0.0.3.1 in the Response to RAI 34, Question 15-3.

**FSAR Impact:**

The U.S. EPR FSAR will not be changed as a result of this question.

**Question 15.06.05-42:**

Although it is possible that the initial core stored energy may not significantly contribute to the PCT, it may have an impact on the SBLOCA core heat transfer characteristics when the break size approaches the upper break size limit of the applicable range of the SBLOCA method. Explain the impact of initial core stored energy on the break size upper limit if the hot rod and assembly are under-predicted by 400 and 350 degrees F respectively, and the inner core region and outer core region by 200 and 100 degrees F respectively. In addition, it appears that boron dilution analysis result during the SBLOCA transient is sensitive to scenario progression through the accident. Discuss the impact of any initial core stored energy under prediction on the result of the boron dilution analysis.

**Response to Question 15.06.05-42:****Part a:**

To assess the impact of the initial fuel stored energy on the small break loss of coolant accident (SBLOCA) transient response, two breaks in the upper size range are analyzed using a higher stored energy. These break sizes are the 8.0 inch inside diameter (ID) break and the 9.71 inch ID break, both located in the reactor coolant pump (RCP) discharge piping. The 9.71 inch ID break represents the largest break size accepted for analysis using the SBLOCA methodology in Reference 1. Break sizes in the upper range are most likely to be impacted by the initial stored energy assumption because their peak cladding temperature (PCT) occurs early in the transient, possibly before the stored energy is dissipated.

The analysis results for these cases are compared to the SBLOCA results presented in the U.S. EPR FSAR Tier 2 for the same break sizes, which assume end-of-cycle (EOC) stored energy and fuel conditions. The analysis results and the comparison between the two stored energy conditions are as follows:

***Fuel Initial Stored Energy and Power Shape Assumptions***

To assess the impact of the stored energy difference that bounds the estimate provided by the NRC (400°F), the RODEX2-2A code was run at beginning-of-cycle (BOC) conditions. The EOC axial shape was used for the RODEX2-2A calculation at BOC to eliminate any axial shape impact on the SBLOCA results. The BOC condition is used only to provide a higher stored energy condition for comparison to the SBLOCA results.

***S-RELAP5 SBLOCA Calculations***

Analyses of the 8.0 inch ID break and the 9.71 inch ID break using the higher stored energy conditions characteristic of BOC fuel exposure show a negligible impact on the transient responses when compared to the results presented in the U.S. EPR FSAR Tier 2 for the same break sizes.

Figure 15.06.05-42-1 and Figure 15.06.05-42-3 show a comparison of the hot rod PCT at the two stored energy conditions for the 8.0 inch and the 9.71 inch ID breaks, respectively. Table 15.06.05-42-1 summarizes the results for these two break cases at the two different stored energies. The system response at the two stored energy conditions show agreement for both break sizes: the hot rod PCT shows an increase of less than 20°F when a higher stored energy

condition is assumed, the PCT occurs at the same axial location and approximately the same transient time for both conditions, and the loop seal clearing pattern is consistent between the two conditions. The 20°F change in PCT is insignificant.

Figure 15.06.05-42-2 and Figure 15.06.05-42-4 show a comparison of the hot rod centerline temperature at peak axial location for the two cases analyzed. Table 15.06.05-42-2 presents a comparison of the peak node centerline temperatures at two times during the transient for the two stored energy assumptions.

The higher stored energy conditions result in higher peak node centerline temperatures by 654°F, 669°F, 582°F, and 426°F for the hot rod, hot assembly, inner core, and outer core regions, respectively. These temperature differences exceed the differences stated in this question, and the analysis conservatively satisfies the request. AREVA NP has not verified NRC's estimate of under-prediction of hot rod and assembly by 400 and 350 degrees F, respectively that is stated in this question. However, these initial temperature differences diminish rapidly to values of 51°F and less at 50 seconds into the transient, prior to the PCT being reached at approximately 365 seconds for the 8.0 inch ID break or 165 seconds for the 9.71 inch ID break (see Table 15.06.05-42-1).

Figure 15.06.05-42-5, Figure 15.06.05-42-6, and Figure 15.06.05-42-7 show the hot rod fuel centerline temperature at several axial nodes adjacent to the peak node. Figure 15.06.05-42-5 illustrates the initial difference in stored energy between the two conditions. Figure 15.06.05-42-6 and Figure 15.06.05-42-7 illustrate the quick dissipation, within 50 seconds, of the stored energy for the 8.0 inch ID and the 9.71 inch ID breaks, respectively.

Even if the initial fuel stored energy used in the U.S. EPR FSAR Tier 2 analyses of the SBLOCA transient is assumed to be under-predicted, its impact on the SBLOCA transient response is negligible because the fuel stored energy is removed before the PCT is reached.

**Part b:**

The impact of the fuel initial stored energy on the SBLOCA boron dilution analysis was assessed.

During the progression of a SBLOCA, a period of natural circulation will occur driven by the core decay heat and stored energy as an energy source and the heat removal by the steam generators (SGs) and the break as the heat sink. Natural circulation is interrupted when voiding in the SG U-tubes is sufficient to block forward circulation of liquid and the secondary system pressure is less than the primary pressure. Under these conditions, the condensate which is reduced in boron content can collect in the primary loops' crossover pipes.

The amount of de-borated liquid accumulating in the SG tubes is dependent on the steam generated due to the heat transferred from the primary system. In the SBLOCA boron dilution analysis, this accumulation of condensate occurs at approximately 500 seconds after the break initiation for the larger break sizes (approximately 4.0 inch ID) and 3000 seconds for the smaller break sizes (approximately 1.5 inch ID). The accumulation of condensate occurs significantly later than the dissipation of the fuel initial stored energy, which occurs between 50 seconds for the larger break sizes and 150 seconds for the smallest break sizes. The only source of heat contributing to the steam generation, and the subsequent condensate accumulation downstream of the SG, is the decay heat and not the stored energy.

Therefore, the stored energy has an insignificant impact on the amount of condensate accumulation in the crossover pipes and consequently on the boron dilution effect.

**References for Question 15.06.05-42:**

1. EMF-2328(P)(A), Revision 0, "PWR Small Break LOCA Evaluation Model, S-RELAP5 Based," Framatome ANP Richland, Inc., March 2001.

**FSAR Impact:**

The U.S. EPR FSAR will not be changed as a result of this question.

**Table 15.06.05-42-1—Summary of Results for SBLOCA Cases at BOC and EOC Exposures**

Break ID	Burnup (GWD/MTU)	PCT (°F)	PCT Node #	PCT Time (sec)	Loops Clearing Time (sec)			
					Loop 1	Loop 2	Loop 3	Loop 4
8.0 inch	0.785 (BOC)	1489	31	366.6	162	162	162	172
	33.8 (EOC)	1470	31	360.2	172	172	172	172
9.71 inch	0.785 (BOC)	1453	31	161.2	100	100	100	100
	33.8 (EOC)	1435	31	165.8	110	110	110	110

**Table 15.06.05-42-2—Fuel Centerline Temperatures for SBLOCA Cases at BOC and EOC Exposures**

Break ID	Burnup (GWD/MTU)	Fuel Centerline Temperature at Peak Node(°F)							
		Hot Rod		Hot Assembly		Inner Core		Outer Core	
		t= 0.0 s	t=50.0s	t= 0.0 s	t=50.0s	t= 0.0 s	t=50.0s	t= 0.0 s	t=50.0s
8.0 inch	0.785 (BOC)	3423	730.81	3359.43	727.1	2535.57	684.95	2123.49	665.3
	33.8 (EOC)	2769	679.55	2690.52	676.6	1953.63	648.84	1698.39	638.05
$\Delta T^1$ (°F)= T <sub>BOC</sub> – T <sub>EOC</sub>		654	51.26	668.91	50.5	581.94	36.11	425.1	27.25
9.71 inch	0.785 (BOC)	3422.34	727.273	3359.43	723.582	2535.57	681.596	2123.493	662.01
	33.8 (EOC)	2768.77	676.193	2690.52	673.253	1953.63	645.619	1698.39	634.884
$\Delta T^1$ (°F)= T <sub>BOC</sub> – T <sub>EOC</sub>		653.57	51.08	668.91	50.32	581.94	35.97	425.1	27.26

Notes:

1. The temperature differences,  $\Delta T$ , at time=0.0s, of 654°F (Hot Rod), 668.9°F (Hot Assembly), 581.94°F (Inner Core), and 425.1°F (Outer Core) are larger than the ones stated in this NRC RAI-167 Question 15.06.05-42.



**Figure 15.06.05-42-1—Hot Rod Cladding Temperature for the 8.0 inch Break**

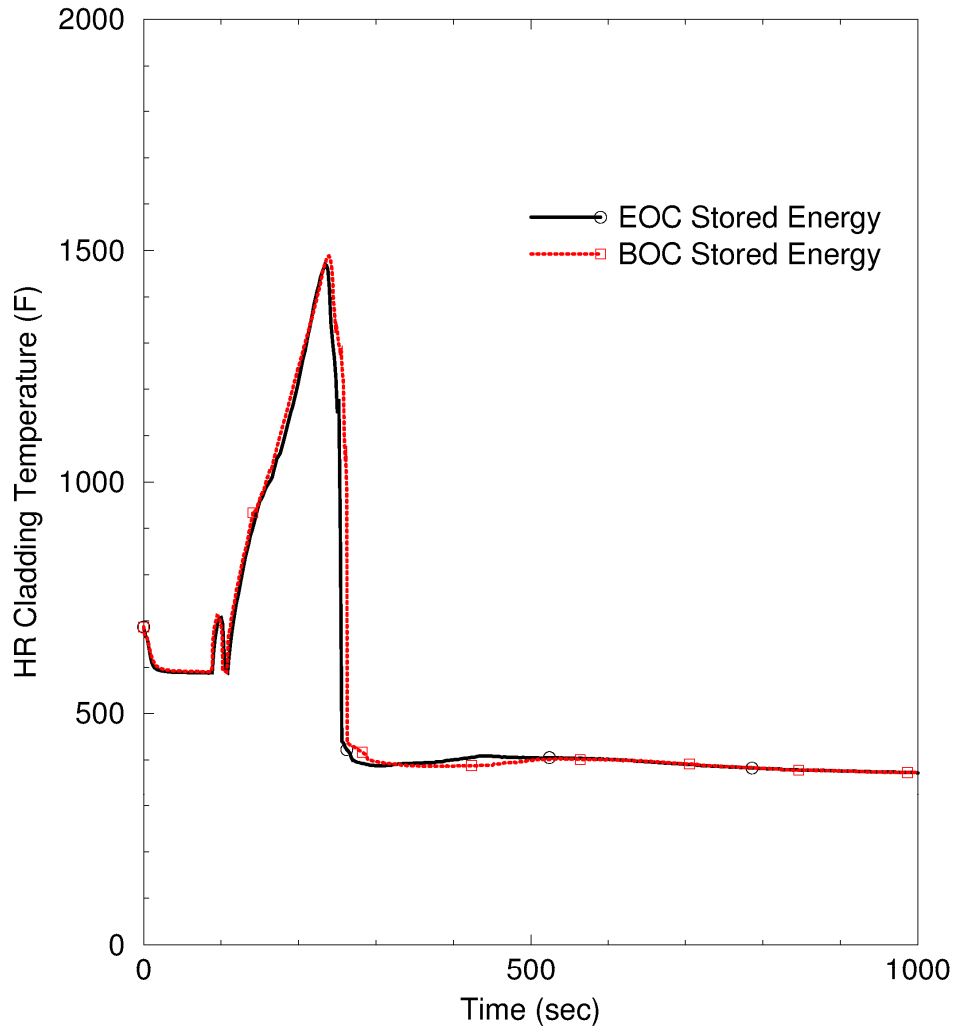
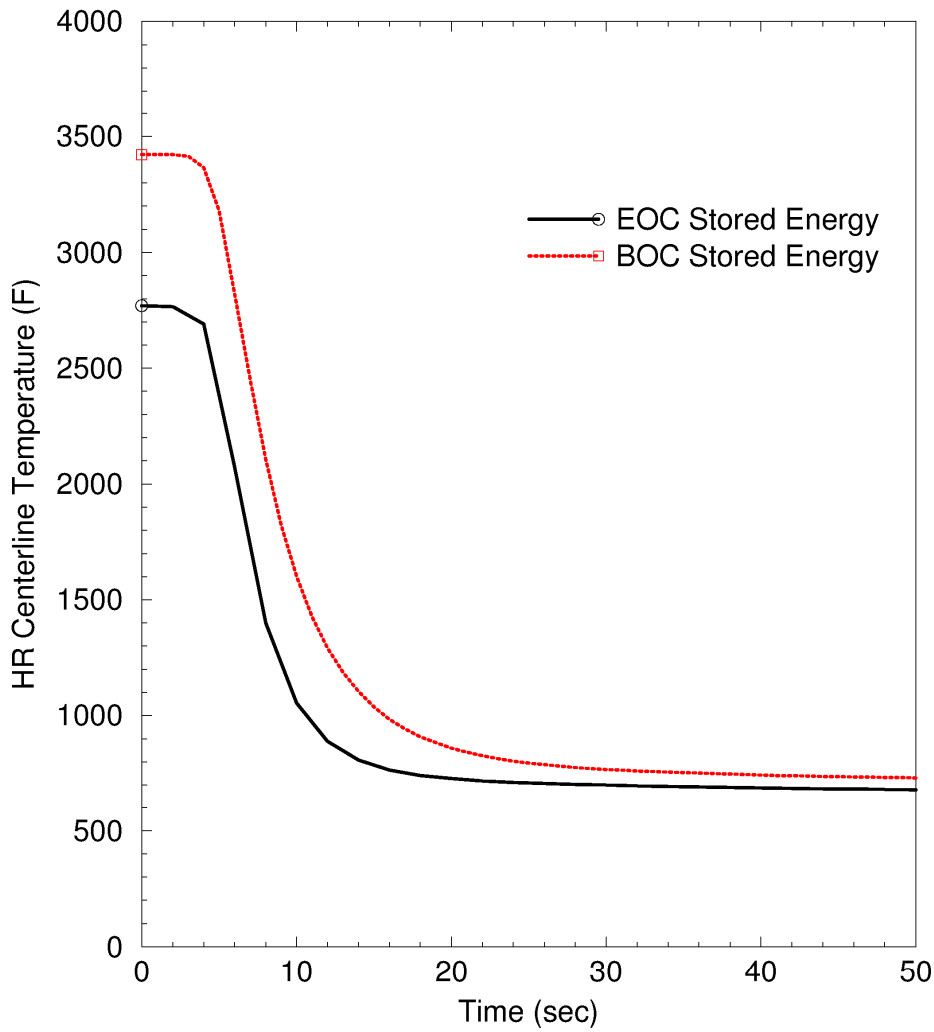


**Figure 15.06.05-42-2—Hot Rod Node 31 Inner Temperature for the 8.0 inch Break to 50s**



ID:12796 2Sep2008 17:44:36 c8in\_003\_acc\_isolated.dmx:1

**Figure 15.06.05-42-3—Hot Rod Cladding Temperature for the 9.71 inch Break**

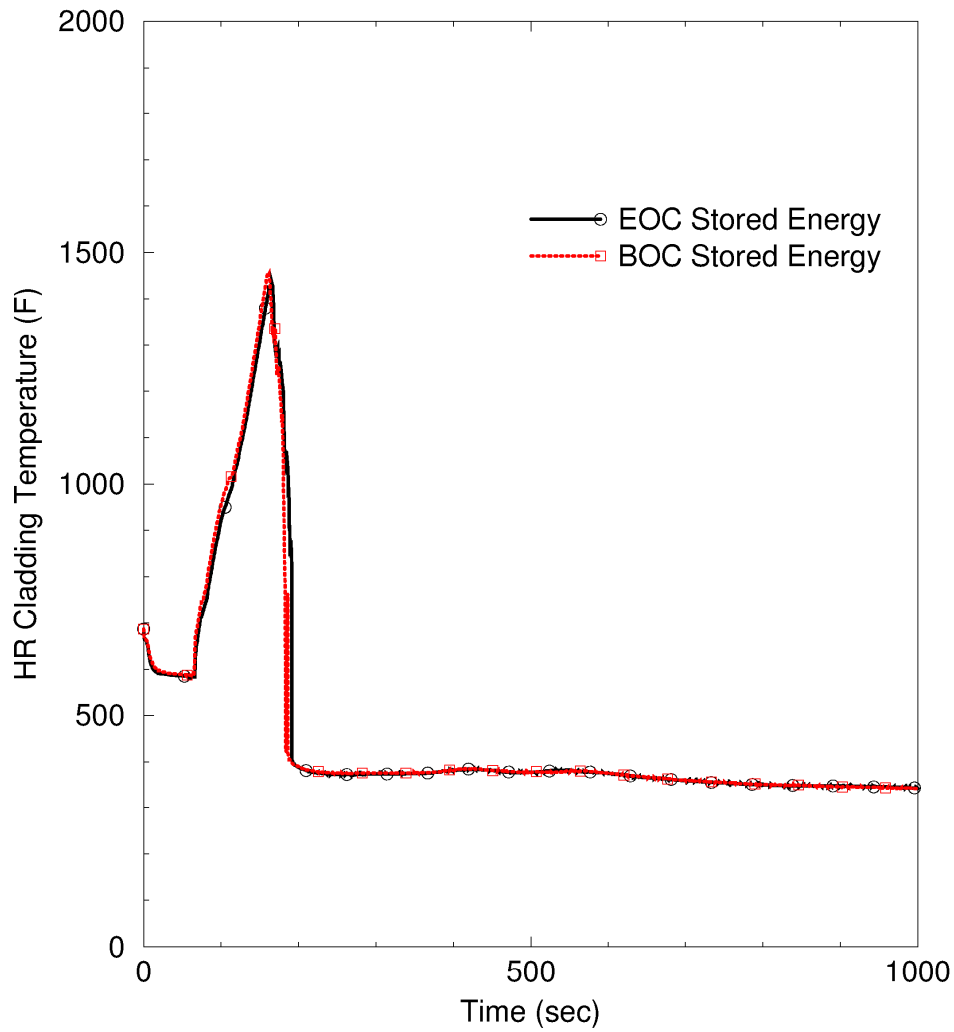


**Figure 15.06.05-42-4—Hot Rod Node 31 Inner Temperature for the 9.71 inch Break to 50s**

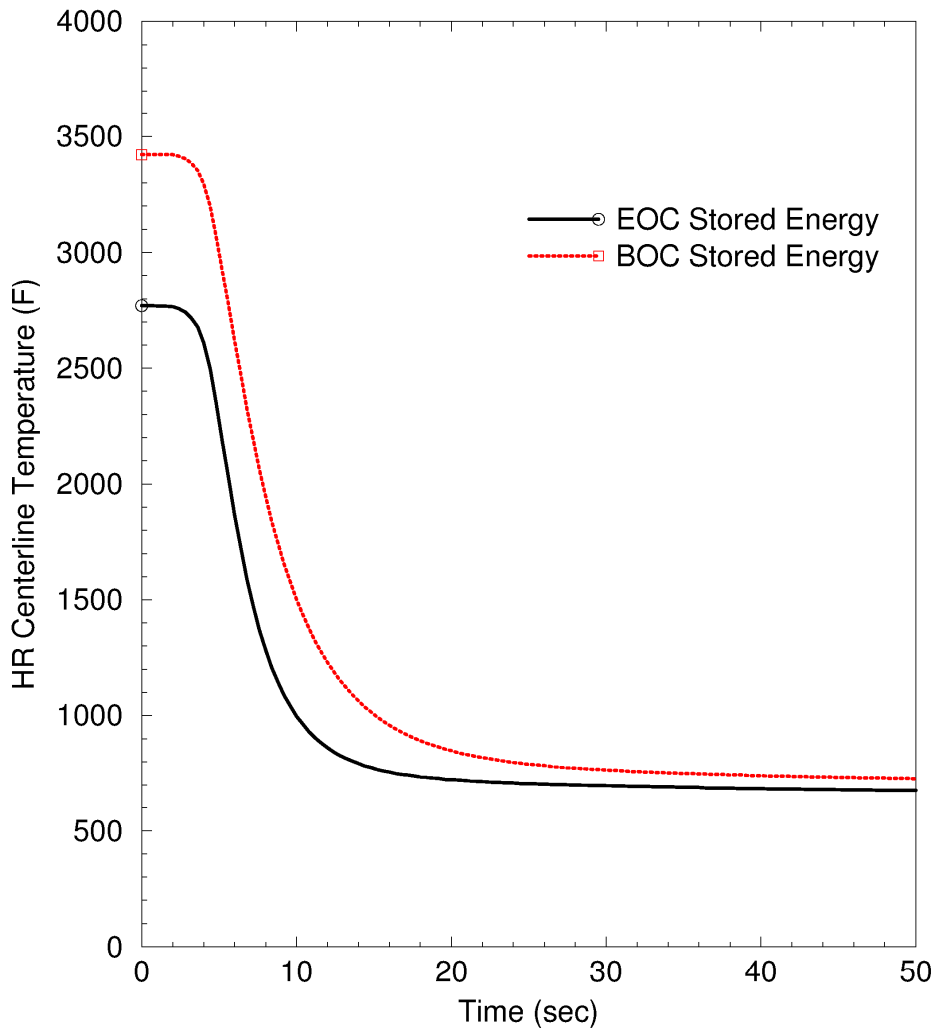


**Figure 15.06.05-42-5—Hot Rod Inner Temperature at 0.0 Seconds**

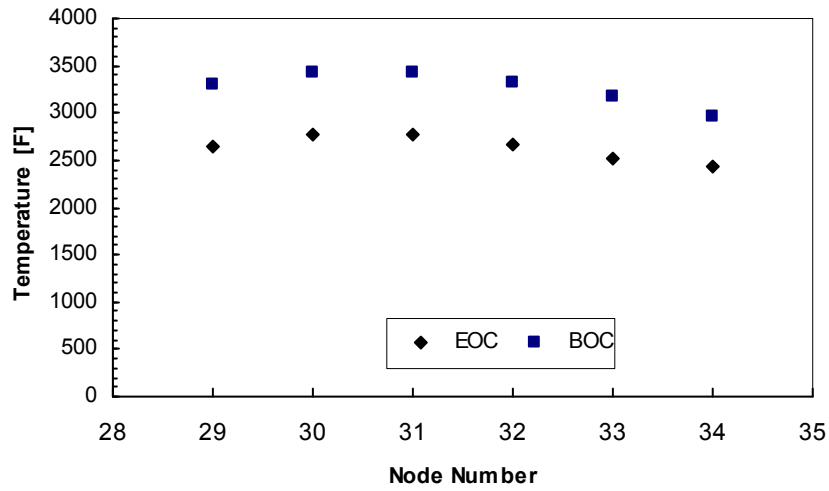


**Figure 15.06.05-42- 6—Hot Rod Inner Temperature at 50 seconds for the 8.0 inch Break**

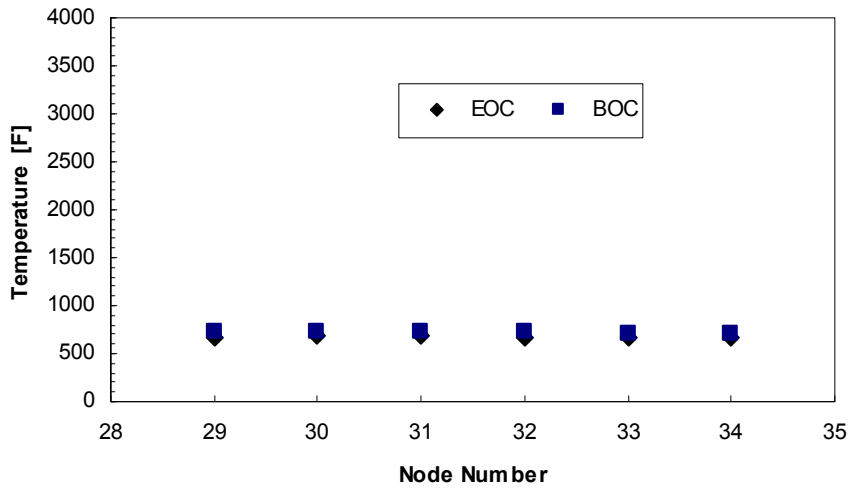


**Figure 15.06.05-42-7—Hot Rod Inner Temperature at 50 seconds for the 9.71 inch Break**

